

A numerical and experimental approach for optimal structural section design of offshore aluminium helidecks

Jung Kwan Seo^{1a}, Dae Kyeom Park¹, Sung Woo Jo², Joo Shin Park^{*3},
Jeong Bon Koo³, Yeong Su Ha³ and Ki Bok Jang³

¹*The Korea Ship and Offshore Research Institute (The Lloyd's Register Foundation Research Centre of Excellence), Pusan National University, Busan, Korea*

²*Department of Naval Architect and Ocean Engineering, Pusan National University, Busan, Korea*

³*Central Research Institute, Samsung Heavy Industries Co., Ltd., Geoje, Republic of Korea*

(Received January 26, 2016, Revised May 2, 2016, Accepted May 3, 2016)

Abstract. Helicopters are essential for supporting offshore oil and gas activities around the world. To ensure accessibility for helicopters, helideck structures must satisfy the safety requirements associated with various environmental and accidental loads. Recently, offshore helideck structures have used aluminium because of its light weight, low maintenance requirements, cost effectiveness and easy installation. However, section designs of aluminum pancakes tend to modify and/or change from the steel pancakes. Therefore, it is necessary to optimize section design and evaluate the safety requirements for aluminium helideck. In this study, a design procedure was developed based on section optimization techniques with experimental studies, industrial regulations and nonlinear finite element analyses. To validate and verify the procedure, a new aluminium section was developed and compared strength capacity with the existing helideck section profiles.

Keywords: safety helideck; nonlinear structural response analysis; optimization; aluminium pancake; accidental load

1. Introduction

Helicopters and helideck structures are generally used to access offshore installations for support and transport in operations and evacuations in fixed and floating platforms and jack-up rigs. The helideck and its supporting structure are critical safety elements due to their functional role in emergency evacuations with potential accidents (fire, explosion etc.). This means, their strength should be satisfied in accidental condition. In general, helideck structures are comprised of deck, girders (or frame) and supporting structures (Fig. 1). A helideck is installed varying type of extruded plank cross-section profile for easy to assembly and installation on offshore structures. Generally, this deck is named “pancake” due to its similarity with a pancake. In the principal design of helideck structures, a safe landing area should be considered for the primary goal. All

*Corresponding author, Senior Researcher, E-mail: jooshin.park@samsung.com

^aProfessor, E-mail: seojk@pusan.ac.kr

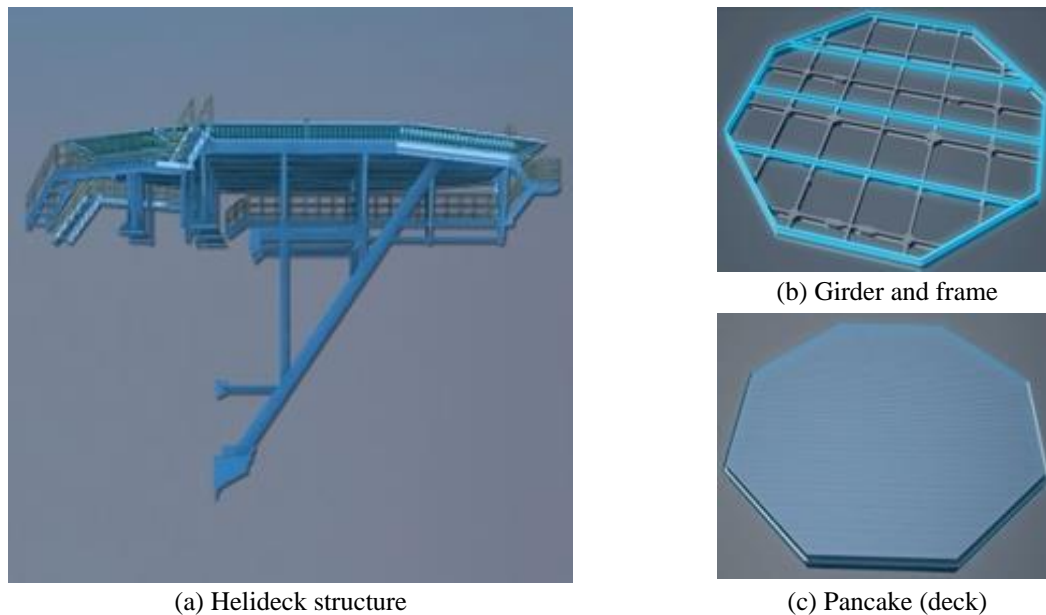


Fig. 1 A typical helideck structure

possible design loads and combinations associated with the environmental and operational information should be considered (Hirdaris *et al.* 2015, Elsayed *et al.* 2016, Raheem 2016). The predominant load on a helideck structure is identified as the impact load induced by a helicopter landing. The helideck structure must also be able to sustain the imposed environmental loads from wind, snow, ice, rotor downwash and personnel, freight, fuel, other temporary equipment, in addition to its own weight (UK CAA 2012, Čokoriloa *et al.* 2013, Park *et al.* 2015). The supporting structure, pancake and girders should be designed to resist the effects of wheel loads acting in combination with other loads in the most extreme location of the structural element being considered. This means that a helicopter should be able to land anywhere within the designated landing area and be parked or stowed anywhere on the helideck.

There are a significant number of regulations governing the use of helicopters and the provision of facilities for their operational fields. These guidelines identify the regulations in force at the time of publication, but users of these documents should always ensure that they refer to the latest issue of any regulation. Over the years, several documents have been published in the form of legal requirements, official notices, guidance and good industry practice for offshore helicopter operations (Mentzoni and Ertesvåg 2015). The current design of offshore helideck structure regulations, codes of practice and relevant official papers and reports are determined by how it is to be operated and the national jurisdiction governing the offshore installations or vessels (HSE 2012).

In generally, classification societies design standards and regulations of helidecks on ships and offshore and installations can be expressed by ISO 19901-3 (ISO 2014), ICAO (ICAO 2013), CAP 437 (CAP 2005), API RP 2L (API 2008), EN1999-1-1 (EN 2007). These regulations describe and specify the offshore helideck structures. The selection of appropriate design codes at the commencement of design is essential to ensure that the helideck structure and support systems are fit for purpose and meet the regulatory and operational requirements.

The available literature on analyses and tests of the ultimate strength of stiffened aluminium plates is limited. Buckling tests on multi-span stiffened plates of aluminium AA5083 were carried out by Clarke (1987). The ultimate strength of stiffened aluminium plates under axial compression (Aalbeg *et al.* 1998) and bi-axial loading was studied using numerical and experimental methods. The results of the experimental and numerical analyses of torsional buckling were presented by Zha and Moan (2000, 2001). Some researchers (Kristensen and Moan 1999, Paik and Buran 2004) have demonstrated the effect of heat affected zones and residual stresses, by investigating the structural behaviour and characterises of aluminium in ship structures. Currently, there are limited published studies of new designs and/or profiles of aluminium helideck structures in offshore installations. A few researchers have considered the structural behaviour of the landing decks of marine vessels (Mascia 2009). It should be necessary to optimise section design methods and evaluate safety requirements for the aluminium helidecks of offshore installations. In the current industrial practices, aluminium pancake designs tend to be based on steel section profile with modifications (Ha *et al.* 2015, Koo *et al.* 2014). The aluminium pancakes are constructed from an extruded 'plank', where severed planks are locked into position to form a pancake assembly. The 'planks' have a built in friction surface, formed by ribs on the extrusion surface. Often, however, good friction values are achieved only in one direction (e.g., across the ribs). Therefore, in the design stages a requirement for the extrusion to be 'milled' across the ribs to obtain adequate friction properties in all directions should be specified (HSE 2012).

This study is the first to develop a design procedure based on optimisation techniques using a preliminary experimental static test, industrial regulations and nonlinear finite element analysis (FEA). To validate and verify the procedure, a new aluminium section profile was developed and the buckling capacities of existing and developed pancakes were compared.

2. Optimal design of aluminium pancake

2.1 Proposed design procedure

Fig. 2 shows a flow chart of a design procedure for an aluminium helideck structure. In the initial stage, the structural shape of the aluminium section profile was investigated using an optimisation technique.

Helideck structures were subjected to multiple loads intended to simulate loading conditions including a live load and a dynamic load such as the impact landing force of selected target helicopters. The optimised aluminium plank section member was then used to code check guidelines and FEA was carried out to validate the optimum design. The evaluations with regard to the structural safety and stability of the developed aluminium pancake were carried out using EN1999-1-1, to comply with the design requirement in this study. For verification, with respect to the evaluation by code, three-dimensional FE analyses were performed.

2.2 Preliminary experimental study

2.2.1 Static loading test on helicopter aluminium planks

The purpose of this test was to understand the structural behaviour of the currently used aluminium pancake profile and to use the results for design of the new plank section member. To determine the initial profile, it should be considered in terms of a selection of widely used

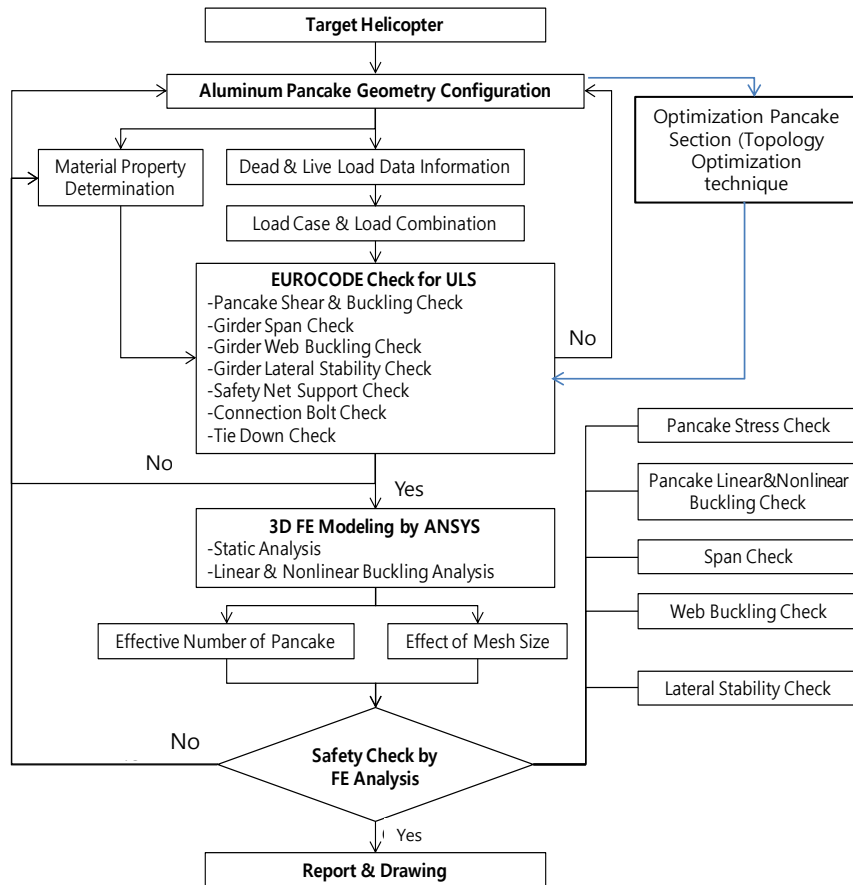


Fig. 2 Flow chart of the design process

aluminium pancakes, with the possibility of expanding to a large size profile and an easily changeable cross section before optimisation analysis. This means of developing new aluminium pancakes provides various benefits, such as ease of installation and maintenance with improving capacity compared to those currently used. Therefore, the initial aluminium pancake profile selected has an easily changeable cross section in the optimisation analysis, making it possible to manufacture an extruded maximum pancake. This preliminary experimental study presents the geometry of the tested pancake module, the test set-up, the test results, which consist of visible observations during the test, and the measured test data. The strength requirement is defined in terms of allowable deflections of the aluminium planks as defined by codes. $L/250$ of limiting values for vertical deflections (deck beams supporting plaster or other brittle finish or non-flexible partitions, where L is span of beam) and 1.0 of applied for calculation in the serviceability limit states were considered (DNV 2011), Nonlinear FE analysis was then undertaken to assess the suitability of the model, and the results were compared with the experimental test results in terms of lateral deflection and load. The FE results can be used as fundamental data to understand the structural behaviour of cross sections and static capacities for the development of new aluminium pancakes.

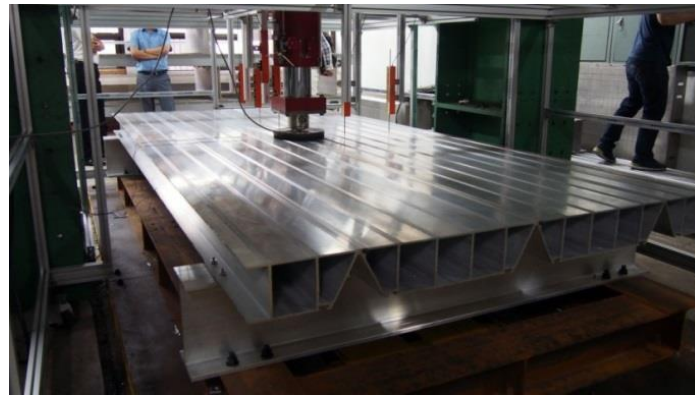
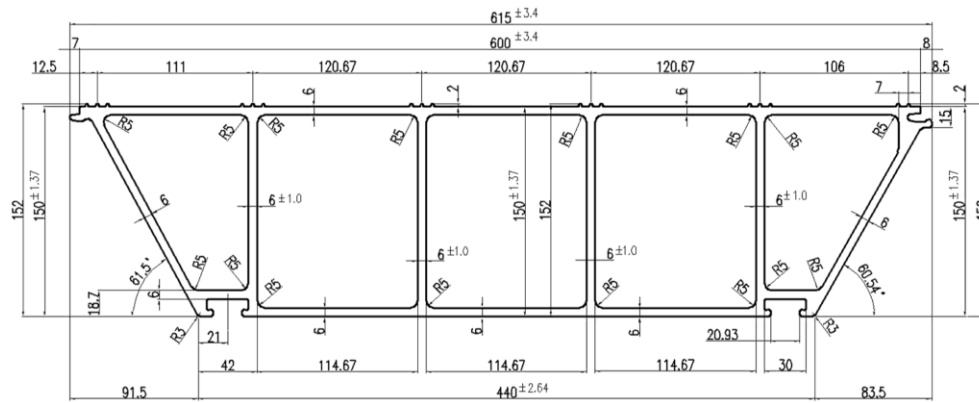


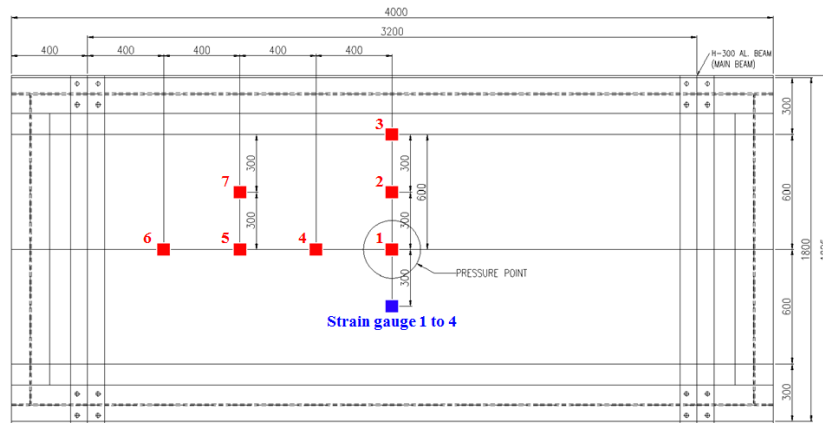
Fig. 4 Test set-up

2.2.2 Geometry and material data

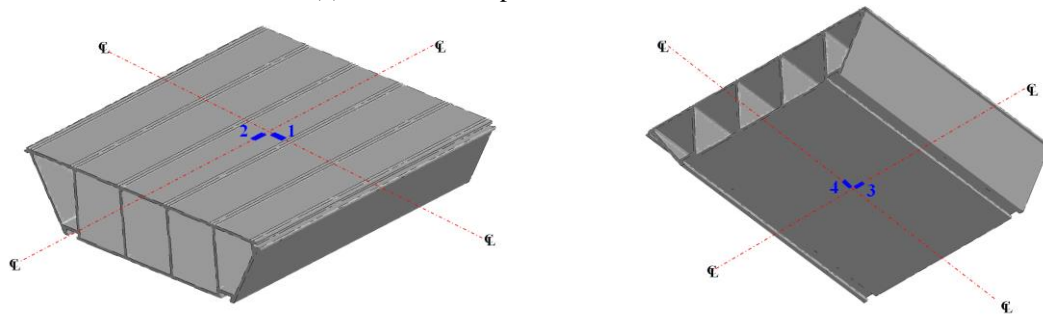
Details of the initial aluminium plank cross-section profile are shown in Fig. 3. The cross section of the pancake is 615×152 mm and the thickness is 6.0 mm. The planks are assembled together, with a length of 4,000 mm and a breadth of 1,825 mm. Two aluminium H-beams (180×300×2,000 mm) were used as supporting members (Fig. 4) with length of 3,200 mm. Clips,

Table 1 Minimum mechanical characteristics

Material	Rp 0.2% (MPa) Yield strength	Rm (MPa) Tensile strength
AL 6082 T6	260	310



(a) Measurement points for lateral deflection



(b) Attachment points and direction for the strain gauges (top and bottom)

Fig. 5 Measurement points for lateral deflection and attachment points for the strain gauges

jointing by bolting were used for the assembled planks to the H-beams. The clips and the shape of the joint are considered, as much as possible, to be realistic of the installation process. Steel H-beams of 200×200 mm support the aluminium H-beams at the bottom. Table 1 shows the minimum material characteristics of aluminium alloy for the planks and H-beams.

2.2.3 Test set-up

The tested planks were supported by a steel frame (Fig. 4). The load was intended to simulate the wheel was transmitted by a steel plate with the same dimension as the tire contact area of $\phi 300$ mm. The thickness of the steel plate was 20 mm. A rubber mat with a thickness of 20 mm was applied between the steel plate and the aluminium planks. A 2,000-kN hydraulic pressure actuator was used to apply the load. The actuator gave a quasi-static load applied at a rate of 0.1 mm/s of speed. A 500 kN load cell, seven Linear Variable Differential Transformers (LVDTs) and four strain gauges measured the load, the lateral deflections and the strains during the test (Fig. 5), respectively. All signals were recorded to a data logger at every 1.0 second. The lateral

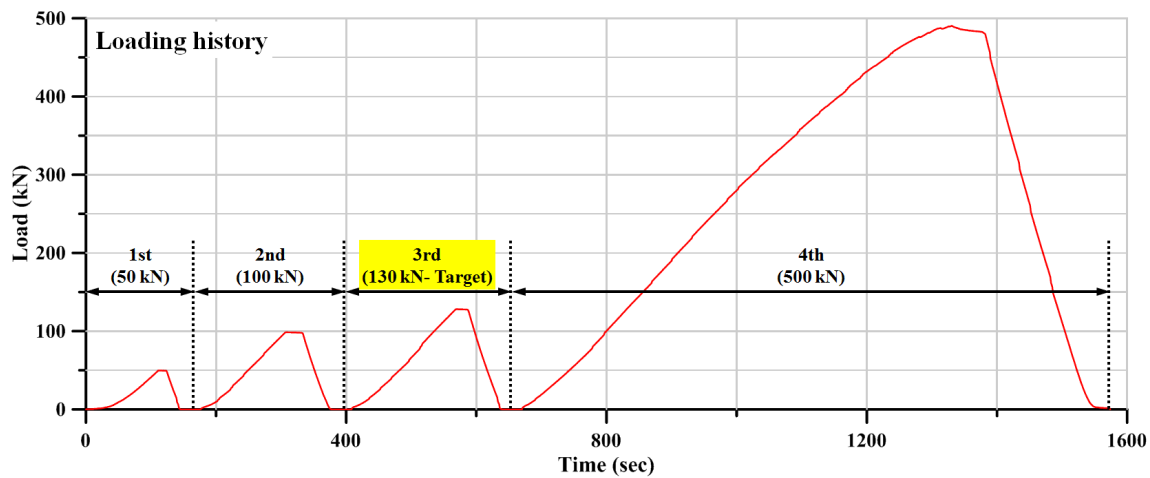


Fig. 6 Load vs. time history

displacements of the planks were measured at seven positions on the test specimen. Two strain gauges were applied at the upper surface next to the tire contact area (distance of 300 mm) and two more strain gauges were applied below on the bottom surface as shown in Fig. 5.

2.2.4 Test procedure

The hydraulic actuator gave a quasi-static loading on the contact area for helicopter wheels until the load reached the target load. Calculation of the maximum take-off mass (MTOM) (approximately equal to 130.0 kN) was assumed with a general helicopter (SIKORSKY S-92) by the DNV code in present test. In total, four load steps were considered, such as 0-50, 0-100, 0-130 and 0-500 kN (Fig. 6). At every local maximum load, the load was kept constant for a short period of time to visually inspect the test specimen.

2.2.5 Test results

Figs. 7 (a) to (d) show test results on the third test of target load (130 kN). The maximum lateral deflection appeared at point 1 and it included the deflection of the rubber pad. Therefore, the maximum lateral deflection should be estimated by using an interpolated lateral deflection at point 1. The interpolation was carried out using three lateral deflection data (points 4, 5 and 6) in the longitudinal direction of test specimen. The maximum lateral deflections were treated as mirrored deflections to draw a global deflected shape (Fig. 9(a) and Fig. 10). The interpolated maximum lateral deflection was investigated at the centre of the length direction. The maximum lateral deflection of the interpolated point 1 reached 6.30, 13.19, 16.82 and 72.57 mm at each target load. The permanent deflections on point 1 were 1.04, 2.02, 1.64 and 13.44 mm after loading.

The strains recorded by strain gauges 2 and 3 indicate axial strain which tend to be tension load. As the load increased, the maximum strains increased. However, they returned to 0.00 until the third loading case (130 kN). In Fig. 7, the result generally tends to be an elastic behaviour, which has an under limit state capacity. It can be observed plastically deformed shape at the local buckling of webs and the bottom surface of planks after the fourth loading case (500 kN) via strain gauges after unloading.

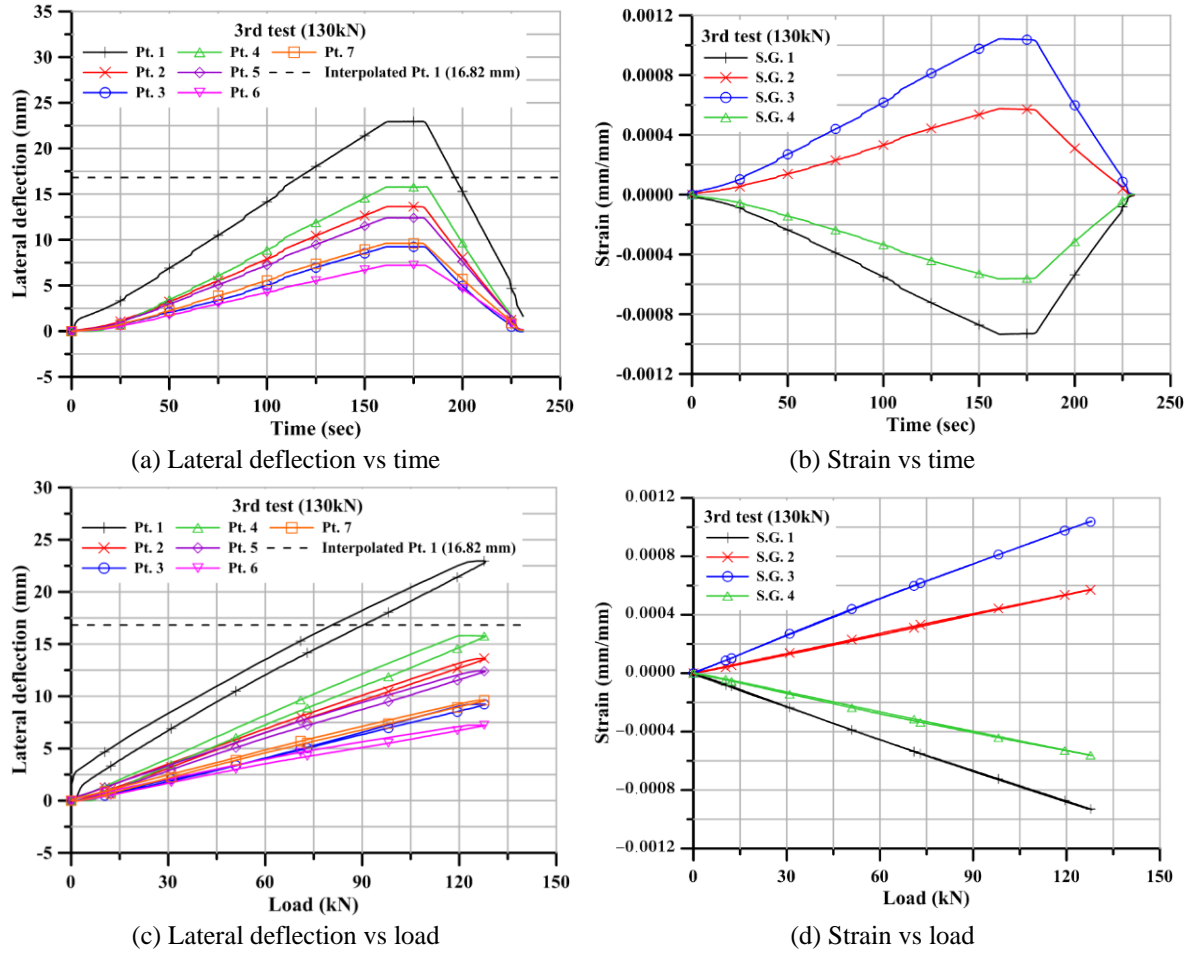


Fig. 7 The test results of the 3rd loading case (130kN)

As expected, the first local buckling was observed at the web of the centre plank at 80 kN of loading (Fig. 8(a)). The linear relationship between the load and time after 80 kN could be combined with the local web buckling and other failure modes. The global deflection showed an arc shape (Fig. 8 (b)) using the testing boundary condition (Fig. 9). The central lateral deflection and loading of the tested planks deflected to the lateral position of end parts upward. It seems that the maximum lateral deflections at the measured points over-detected the expected criteria ($L/250=12.80$ mm) due to the risen end parts of the specimen.

Fig. 10 shows a raised end part of the tested plank, which was estimated by the interpolation of the real test results. Points 4 to 6 are central points in the length direction at 400, 800 and 1200 mm distances from the loading point. The maximum deflection of points 4 to 6 mirrored the estimate of the second order polynomials. From the equations, 2.74, 7.80, 9.97 and 53.66 mm of the lateral deflection was increased at the end of the planks (Fig. 10). A real deformed shape (boundary condition) corresponding to the real (continued boundary condition which is a part of whole planks) installation is shown in Fig. 9(b). The maximum lateral deflection would be decreased by using proper supporting members (Fig. 4). According to Fig. 10, the condition of end parts (0 mm

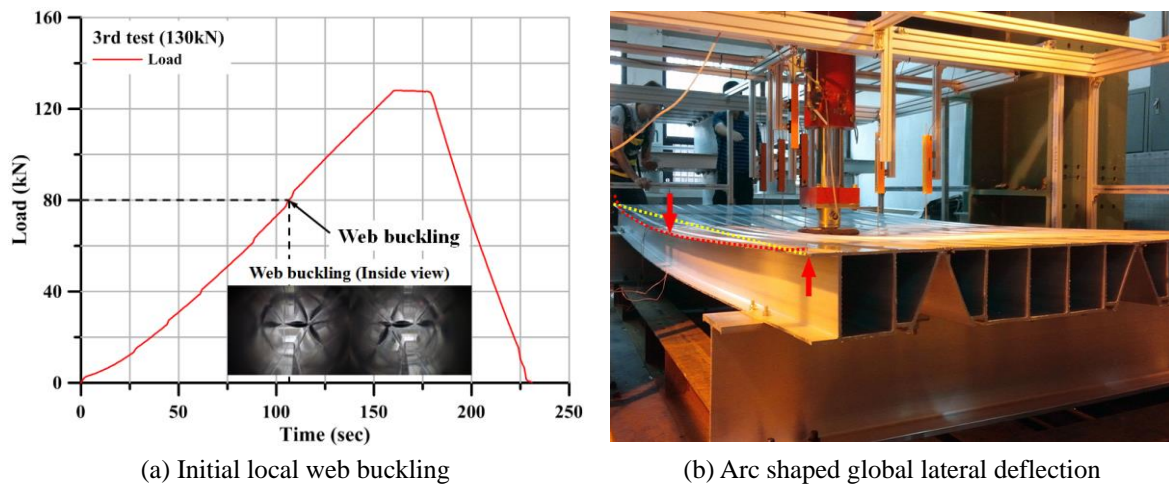


Fig. 8 Local buckling and global deflection

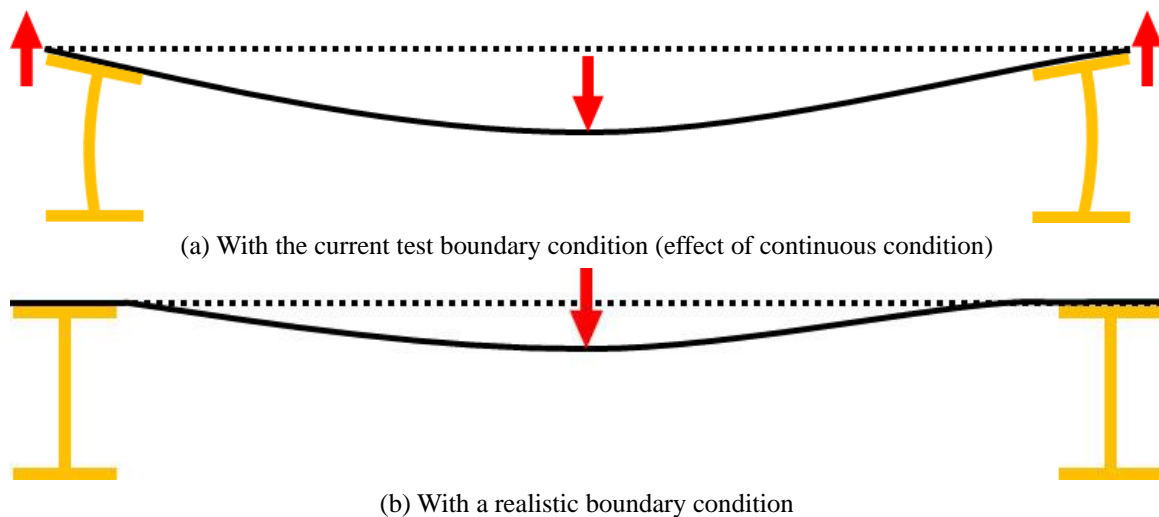


Fig. 9 Global lateral deflection with the effects of boundary conditions

and 4,000 mm) tended to be a simply support condition. Therefore, the maximum lateral deflection was over deflected (16.82 mm at interpolated lateral deflection (Point 1) and criteria: 12.8 mm ($L/250$)). This means that the boundary condition in the present test affected the increased lateral detections with the initial lateral deformations.

From the results of present tests, a large-scale test with proper supporting members (Fig. 4) is highly recommended to achieve accurate results. For load carrying capacity, the capacity of the large planks was good enough based on the results of the current load vs. the deflection curve (Fig. 7). This initial profile will be applied in optimisation analyses of a new section profile.

2.2.6 FE simulation

An FE simulation was performed on the preliminary experimental test. The aluminium planks

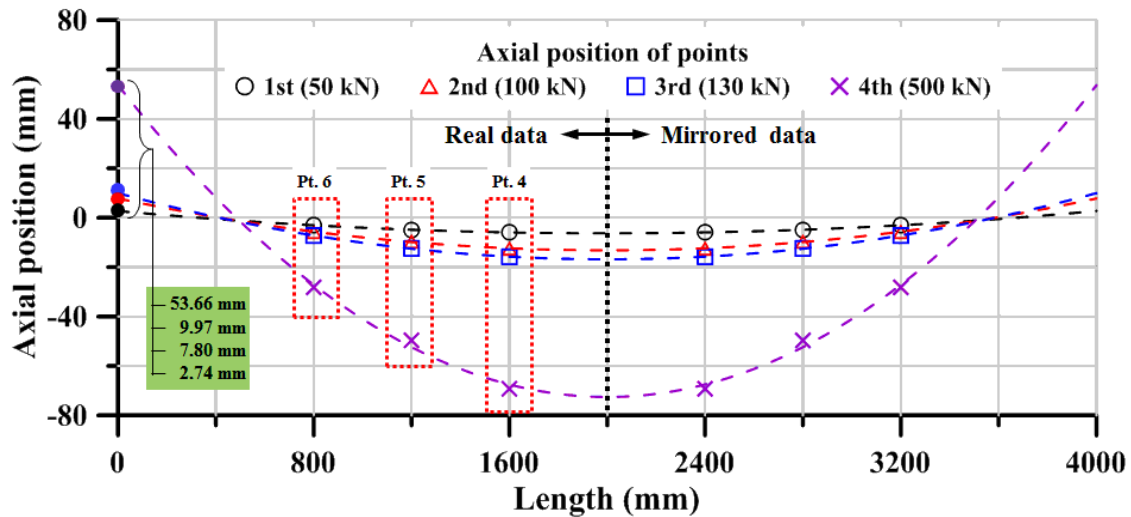


Fig. 10 Lateral deflection estimation with an arc-shaped global lateral deflection

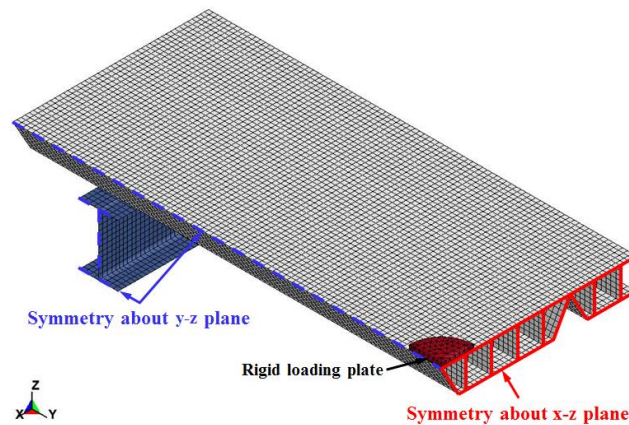


Fig. 11 An FE model of the preliminary experiments

and the aluminium H-beam parts were considered. A quarter model was used due to the symmetric condition of the test specimen. The test model in Figs. 3 to 5 was modelled with four-node shell elements, as shown in Fig. 11. The aspect ratio of the elements was about 1.1. A rigid solid element acted as the steel loading plate in the experiments, with a quasi-static loading on the planks. Symmetric boundary conditions were applied to the symmetric plane of the model, and three-dimensional translates were constrained on the contact area between the aluminium and the steel H-beams. FE material modelling based on the material tensile test was performed using the Ramberg-Osgood equation. The FE analysis reflected the experimental test setup well using proper FE techniques. Similar assumptions and FE techniques were also used for further analyses.

Figs. 12 and 13 show the FE analysis results for the 3rd test (130 kN). Fig. 12 shows that the lateral deflection in the FE analysis and in the experiment was similar. Not only was the stepwise lateral deflection of the aluminium pancakes observed, but the risen ends of the aluminium planks were also seen, similar to Fig. 9(a). Fig. 13 shows a comparison of the lateral deflections in the

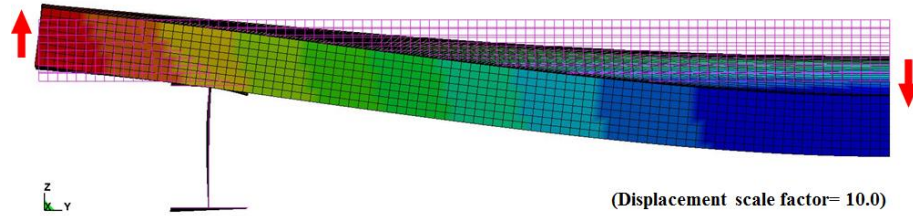


Fig. 12 Lateral deflection contour of the FE analysis for the third test (130 kN)

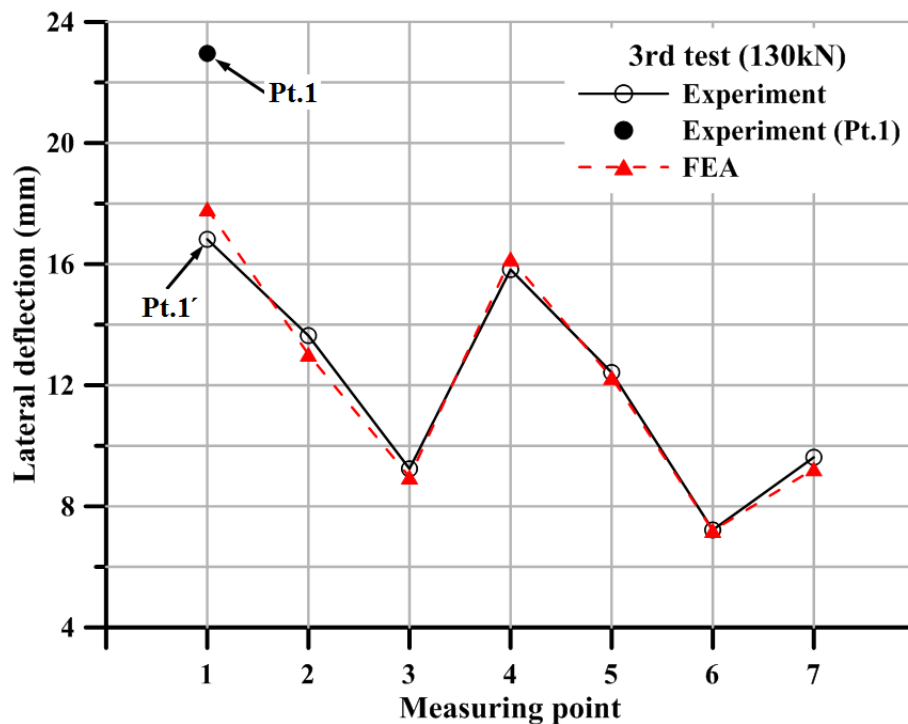


Fig. 13 Lateral deflections of the experiment and the FE analysis for the third test

experiment and the FE analysis at each deflection measuring point. The difference between the experiment and FE analysis results was less than 1.0 mm at point 1, which was estimated using a polynomial equation in Fig. 10. The difference between points 1 and 1' is most likely due to the rubber pad used in the experiment. Measurement point 1 is at Rigid loading plate as shown in Fig. 11. It is highly difference between FEA and Experiment because it is included in thickness of Rigid loading plate. Morst results is very well matched with FEA and Experiment results. Also local buckling of the pancake in Fig. 8(a) was also observed.

2.3 Details of target helicopter

Many types of helicopters are available in offshore industries considering the size of the platform, the function of the helicopter and etc. However, the target helicopter in present study was a EUROCOPTER (now Airbus Helicopters) AS332 L2 with a weight of 9,300 kgf and a

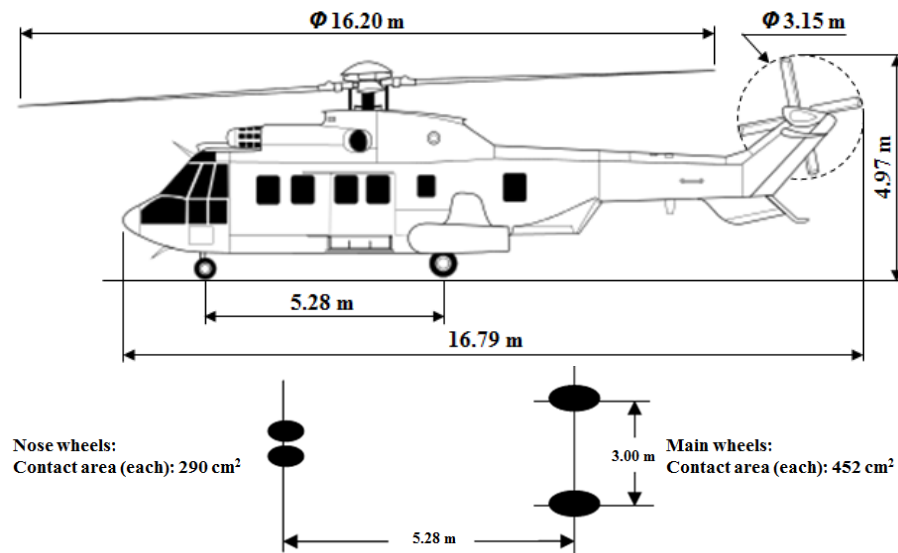


Fig. 14 Dimensions of EUROCOPTER AS332 L2

Table 2 General design data

Overall Length	19.5 m	Landing Net size	Medium 12 x 12 m
Max. All up weight	19,300 kg	Passenger Access	Sliding main cabin door both slides
0.83D obstacle Limit Dimension	16.19 m	Refuelling Method	Pressure and gravity
0.62D obstacle Limit Dimension	12.09 m	Refuelling point location	2 gravity fill points on starboard side pressure fill point on starboard side
0.12D Inner Limit Dimension	2.34 m @ height 975 mm	Fuel type	Jet A-1
0.21D Outer Limit Dimension	4.09 m @ height 975 to 3,022 mm	Max. Fuel load	4,180 lbs (2,406 l)
Minimum Foam Application Rate	1,643 l/min	Undercarriage	Tricycle

diameter of 19.5 m. The helicopter is a four-bladed, twin-engine, medium-sized utility helicopter developed and marketed by Aerospatiale and Eurocopter (Wikipediz 2016). Fig. 14 and Table 2 show details of the target helicopter design data for optimisation of the aluminium helideck.

2.4 Optimisation analysis

This section describes the optimisation of the cross section of the aluminium pancake structure during emergency landing situations and verification of the optimised model. For more stiff and cost-neutral aluminium pancake structures, an optimisation may be considered in offshore and marine industries.

Topology optimisation has traditionally been used to determine the optimum material layout of

a structure. The aforementioned optimum is in general defined as that which minimises an objective function while satisfying a number of designer-imposed constraints.

A common objective is the minimisation of the material volume of the structure, while ensuring a number of designer-imposed stiffness constraints (often in terms of limits on the maximum deflection of the structure or strain energy, i.e., compliance). Also, out of many available optimization algorithms, classical approach to the numerical solution of a discretized structural optimization problem is the optimality criteria method. Optimality criteria method is very efficient for solving the topology optimization method. Optimality criteria method is used in various fields of engineering application as a very strong method of optimization (Shukla and Misra 2013). These problems are generally formulated in a deterministic setting under static load distributions, notwithstanding the inherently uncertain and time-dependent environment in which the structures are generally set. In this study, the optimisation of the aluminium pancake structure was performed using the TOSCA Structure code, which is based on optimality criteria method for solving topology optimisation method (TOSCA 2012). The TOSCA Structure method is the most refined method currently available and is believed to provide the most accurate and practical solutions. The generation of FEA models and the stress evaluations are conducted using FEA code (NX Nastran 2012),

2.4.1 Design condition

In emergency landing situation of a helicopter, a specific loading is applied to the area on the pancake. The loading value (the same as patch loading according to the target helicopter) is 21.15 ton and the uniform loading is applied on the $300 \times 300 \text{ mm}^2$ (Fig. 15).

The loading cases for the optimisation are considered as four loading cases according to the position of the patch areas. Two loading conditions on top of pancake and two loading conditions which are a possible emergency landing situation are considered, as shown in Figs. 16(a) to 16(b). The aluminium pancakes are supported by two girders with 4,500 mm of length and 4,800 mm of width. The bottom of the girder is fixed in all degrees of freedom (DOF) as shown in Fig. 16(b).

All of the aluminium pancakes and girders are considered as AL 6082 T6. The detailed properties of AL 6082 T6 are modelled by the Ramberg-Osgood equation with the minimum requirements for mechanical material properties from EN1999-1-1, shown in Fig. 17. The allowable stress of AL 6082 T6 can be calculated using Eq. (1).

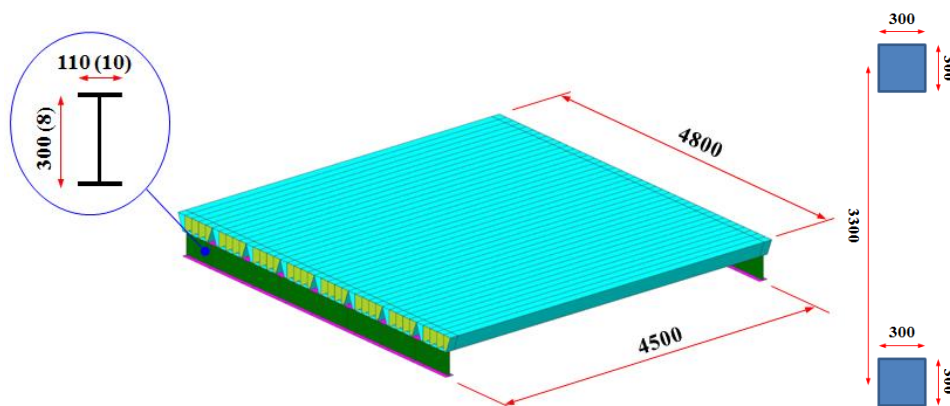


Fig. 15 Base structure shape of helideck (left) and patch loading area (right)

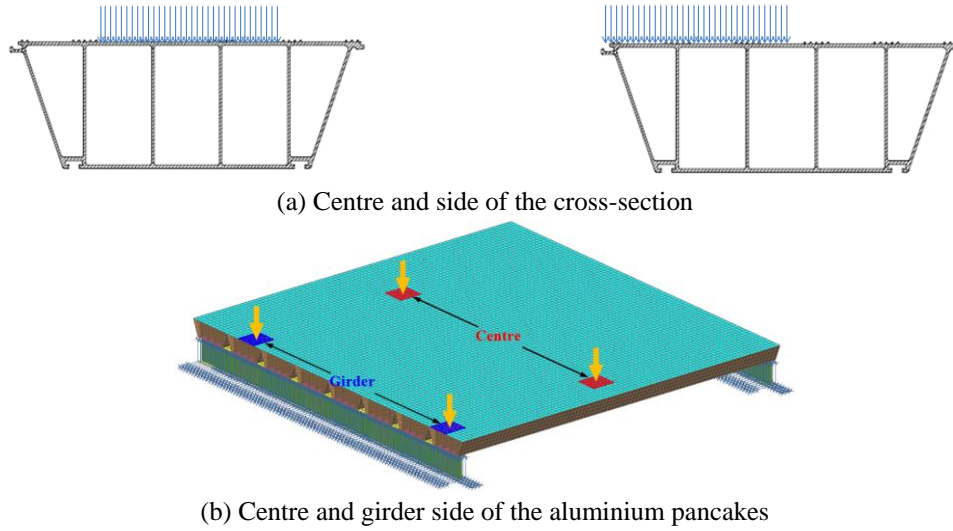


Fig. 16 Patch load location

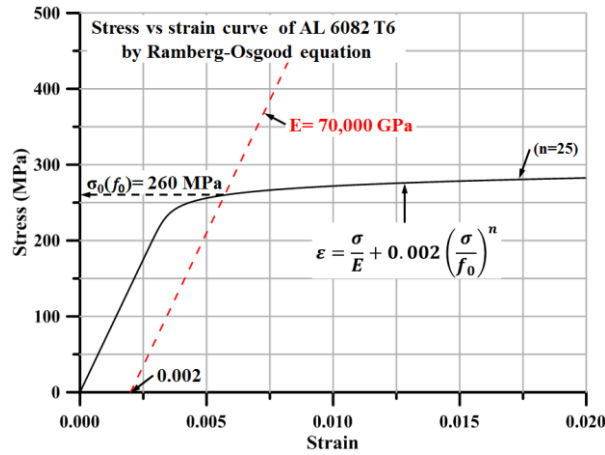


Fig. 17 Material constitutive curve of AL 6082 T6

$$\sigma_{allow} = \text{Peak stress effect} \times \text{ALS condition} \times \text{Yield stress} \quad (1)$$

2.4.2 Optimization condition

A simplified optimisation model representing the preliminary test result was used to optimise the aluminium cross section model. The cross section details and loading and support conditions used in the current industrial study are based on static load carrying capacity. The objective of this optimisation was a maximisation of the stiffness (minimisation of the sum of the strain energy) of the pancake with a volume constraint. The design variables are all plate elements in the section except for an outline of a non-design variable. Three different cross section cases of aluminium pancake were considered in this optimisation. The dimensions and section properties of each pancake are shown in Table 3.

Table 3 Details of optimization cases

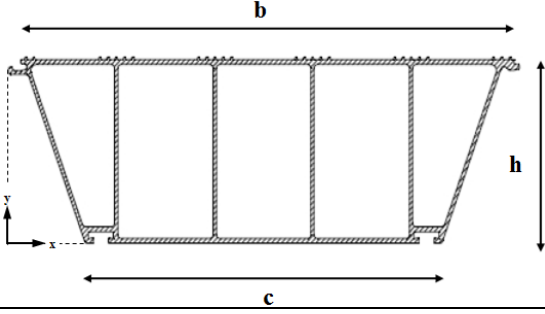
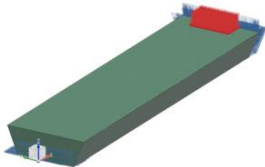
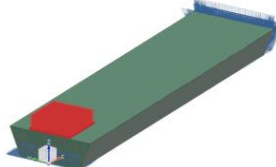
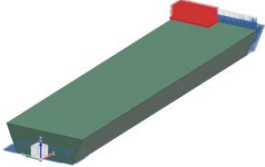
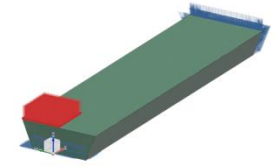


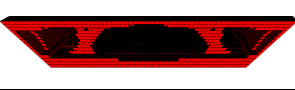
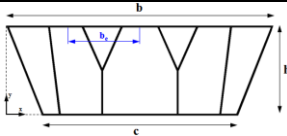
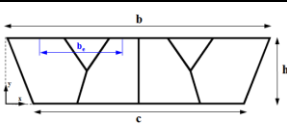
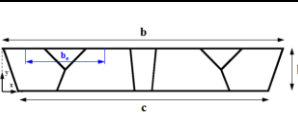
Cross-section parameters			
			
Case	Case I	Case II	Case III
b [mm]	600.00	600.00	650.00
c [mm]	440.00	480.00	580.00
h [mm]	200.00	150.00	100.00
Area [mm ²]	8.12E+3	7.24E+3	6.83E+3
Slenderness (Flange/Web)	29.10/64.00	31.80/47.30	39.80/32.00
Moment of inertia about the x axis (I_{xx}) (mm ⁴)	4.96E+7	2.58E+7	1.17E+7
Moment of inertia about the y axis (I_{yy}) (mm ⁴)	2.44E+8	2.19E+8	2.46E+8
Centroid position along x axis (mm)	300.00	300.00	325.00
Centroid position along y axis (mm)	106.93	79.08	51.81

Table 4 Loading conditions for optimization analysis

Patch	Section	ID	Loading conditions	Patch	Section	ID	Loading conditions
Centre	Centre	CC		Girder	Centre	GC	
	Side	CS			Side	GS	

Topology optimisation has been repeatedly used to consider the loading and constraints of each case to find the optimised cross section. Table 4 shows the four loading conditions mentioned above, tabulated as varying loading cases for applied loadings. The objective and constraints of this optimisation task are maximum stiffness and X-Z plane mirror, symmetric, volume ($<< 25\%$).

Table 5 Optimization results and defined initial cross-section

Case	CASE I	CASE II	CASE III
Optimization Result			
Optimized section			
b (mm)	600.00	600.00	650.00
c (mm)	440.00	480.00	580.00
h (mm)	200.00	150.00	100.00
Area (mm ²)	8.96E+3	6.97E+3	6.79E+3
Slenderness (Flange/Web)	38.01/48.00	39.00/28.00	37.67/18.00
Moment of inertia about the x axis (I_{xx}) (mm ⁴)	5.16E+7	2.51E+7	1.16E+7
Moment of inertia about the y axis (I_{yy}) (mm ⁴)	2.63E+8	1.96E+8	2.40E+8
Centroid position along x axis (mm)	300.00	300.00	325.00
Centroid position along y axis (mm)	110.80	82.77	53.57

2.4.3 Optimization results

Table 5 shows the optimisation results and initially optimised cross section shapes for each case analysed using the TOSCA Structure method. The results of analysis involved the determination of features, such as location and shape of holes, and the connectivity of the domain. After the topology optimisation, the design model is no longer purely based on geometrical data. Therefore this rough design proposal must be smoothed and reshaped. The results were used to determine the basic layout of a new section.

To verify the optimisation results, optimised cross sections were generated as three-dimensional models and the structural stabilities of each result was evaluated using FEA. By repeating the optimisation analysis, the final three optimised cross section cases could be considered as comparison targets (Table 6). To evaluate the structural stabilities of the cross sections, optimised models were analysed and compared with each case individually. The maximum von-Mises stress, lateral displacement and weight were compared.

Topology optimisation was performed using repeating iterations to find the optimised cross sections of the aluminium pancakes and these were verified using FEA to check structural stabilities. All three cross sections should be satisfied their maximum stiffness with a volume constraint, stress, displacement and weight (Table 6) within range of initial capacities of section profile. Fig. 18 represents the efficiency of the results by comparing the stress, displacement and weight results of each case.

Table 6 Final optimized sections and finite element analysis results

	Case	Case I	Case II	Case III
CC	Stress (MPa)	340.1	475.3	674.6
	Disp. (mm)	51.76	68.16	127.60
CS	Stress (MPa)	319.1	462.7	654.4
	Disp. (mm)	53.42	71.74	122.90
GC	Stress (MPa)	253.2	530.7	531.8
	Disp. (mm)	4.69	4.21	7.48
GS	Stress (MPa)	245.0	535.2	527.1
	Disp. (mm)	4.56	4.31	7.26
Weight per 1 m (kg/m)		25.5	25.3	25.6

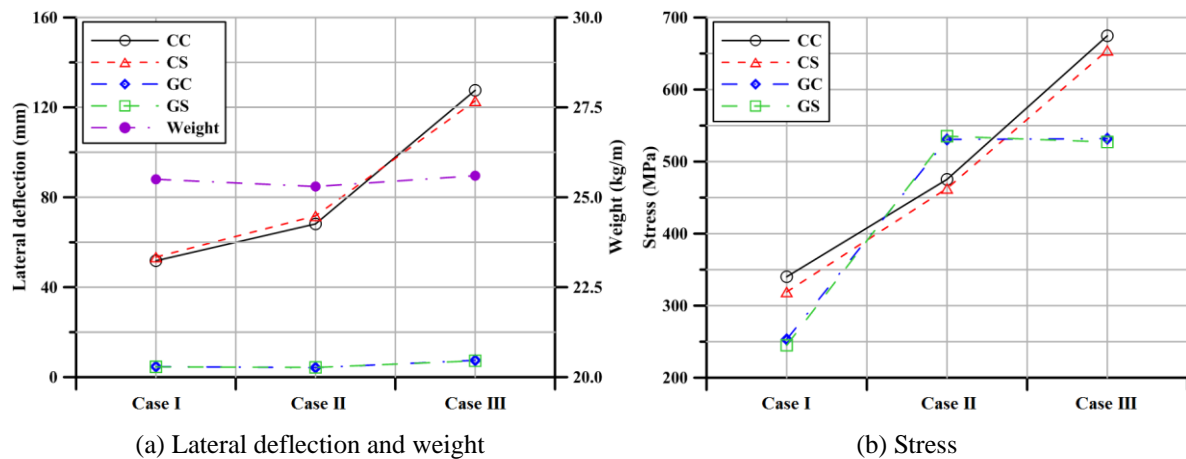


Fig. 18 Comparison of the lateral deflection, weight and stress results in each case

The objective of this optimisation task was to maximise stiffness with a volume constraint. Case I shows the best solution in the comparison with the other cases. The section properties of the developed cross section for an aluminium pancake according to the optimisation results are shown in Table 7.

3. Evaluation of codes and nonlinear FE analysis

3.1 Determination of accidental loads

In an emergency landing of helicopter, an impact load of 2.5 times the maximum take-off weight (MTOW) could be applied on any position of the landing area and a structural response factor of 1.3 should be used unless further information allows a lower factor to be calculated by CAP437. The helideck and its supporting structures should be designed to resist concentrated horizontal imposed loads equivalent to $0.5 \times \text{MTOW}$ of the helicopter, distributed between the undercarriages in proportion to the applied vertical loading in the direction which will produce the

Table 7 Section properties of the developed pancake

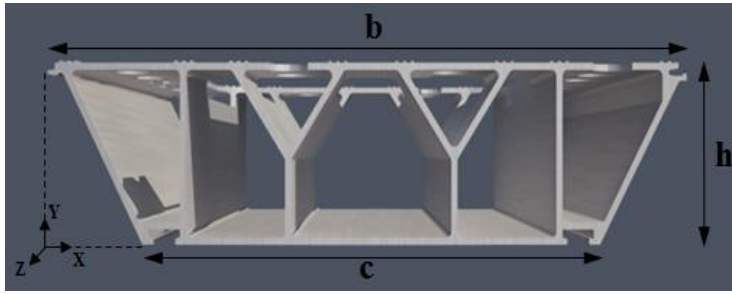
Developed aluminium pancake profile	
	
b [mm]	615
c [mm]	440
h [mm]	150
Area [mm ²]	9,012
Moment of inertia about the x axis (I_{xx}) (mm ⁴)	3.10E+7
Moment of inertia about the y axis (I_{yy}) (mm ⁴)	2.68E+8
Centroid position along x axis (mm)	304.00
Centroid position along y axis (mm)	83.00

Table 8 Yielding and shear buckling check for one web of pancake

Yielding Check		Shear Buckling Check	
V_{Rd}	95.52 kN	V_{Rd}	347.71 kN
Net Effective Area (A_{net})	700 mm ²	Reduction factor (v_1)	1.456
Partial Safety Factor (γ_{M1})	1.1	Partial Safety Factor (γ_{M1})	1.1
Safety Check (V_{ed}/V_{Rd})	0.107 (≤ 1.00)	Buckling coefficient (k_t)	37.37
		Safety Check (V_{ed}/V_{Rd})	0.029 (≤ 1.00)

most severe loading on the element being considered. Therefore, the loads induced by helicopter landing can be calculated as a vertical impact load of 296.5 kN, a maximum landing force per wheel of 148.3kN and a lateral impact load of 45.6kN.

3.2 Regulation design code for structural safety evaluations

The evaluations with regard to the structural safety and stability of the developed aluminium pancake were carried out using EN1999-1-1 to comply with the design requirement. The design shear resistance for both yielding and buckling should be checked, as the slenderness parameter, β , of the pancake is greater than 39.0. The design shear force acting on one web of aluminium pancake was determined by considering the effective number (V_{ed}) of the aluminium pancake verified by FEA. The design shear force was taken to be concentrated force for one web of 74.13 kN, distributed force for one web of 0.002 kN and design shear force (V_{ed}) of 74.15 kN, according

to EN1999-1-1. The yield and shear buckling check results for the web of the aluminium pancake are indicated in Table 8.

3.3 Nonlinear structural FE analysis

3.3.1 FE analysis of the AL pancake

Simulation of the actual structural behaviour of the developed aluminium pancake requires several considerations. As the thin plate elements of the plate stiffened panel structures are subjected to local and global buckling, while the plate and stiffener are subjected to in-plane and out of plane buckling effects, the chosen element must be capable of modelling these buckling phenomena and the associated behaviour. It must be capable of modelling the structural behaviour both in linear and nonlinear regions involving large displacements, elasto-plastic deformations and associated plasticity effects. In the NX Nastran element library, the shell elements generally satisfy these criteria and can be used to model the plate elements of plate-stiffened panels. Although there are different types of shell elements available in the element library, the three-dimensional thin iso-parametric quadrilateral shell element with four nodes and six DOFs per node was used to model the steel plate element, as it was considered the most suitable for the proposed FEA. A material constitutive curve using the Ramberg-Osgood law, based on the minimum requirements of the material (AL 6082 T6) was applied for the aluminium pancake, as shown in Fig. 17.

3.3.2 Boundary conditions and load conditions

For the present nonlinear FEA, the helideck planks model was applied in the span length (x) direction to accurately account for the effects of the rotational restraints along the edges (y), as described in Fig. 19. This model is suitable for the geometric properties and structural behaviour of the panel considered here because its panel deflection behaviour is symmetric between girders. In this study, we used one extreme edge condition, namely, simply supported, along the longitudinal edges (or at the bottom girders), as shown in Table 9.

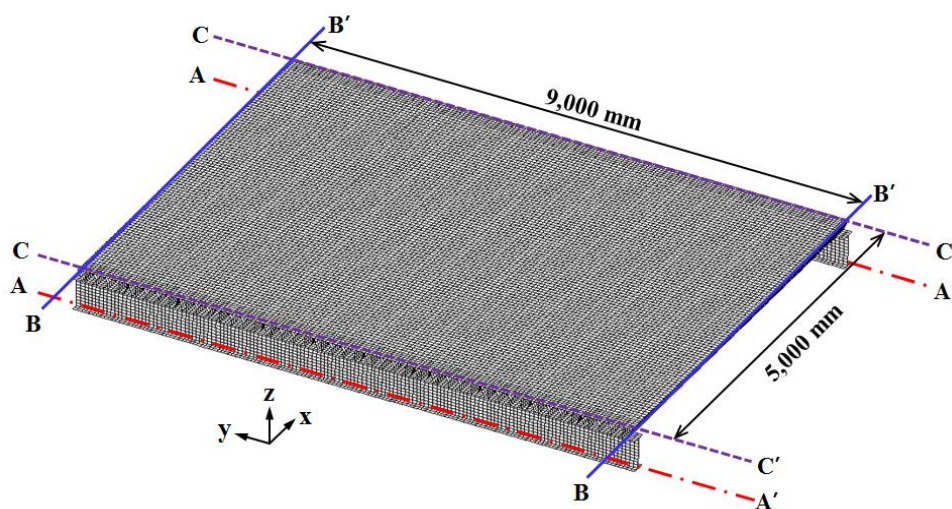


Fig. 19 FE model of the aluminium pancake with H-beam girders

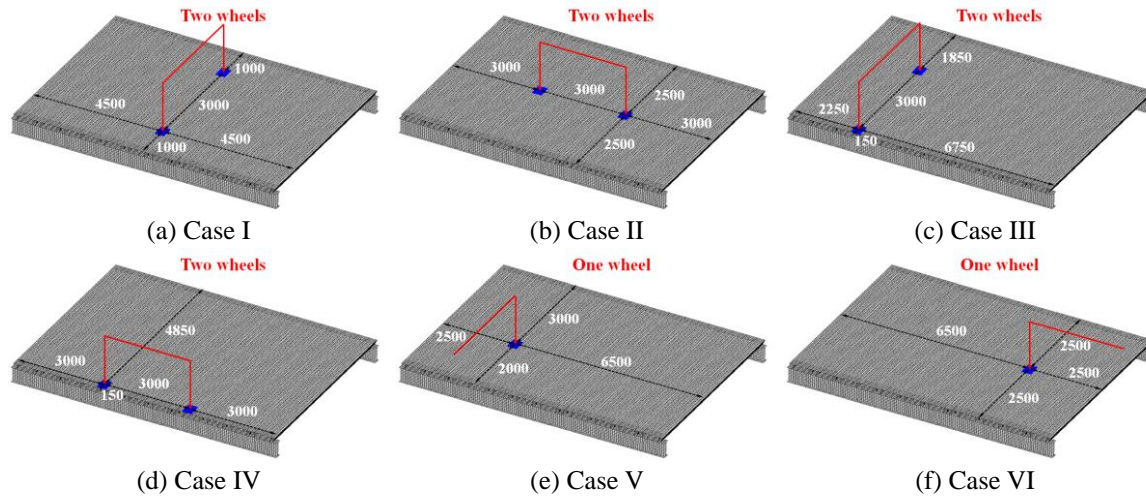


Fig. 20 Load cases for FE analysis

Table 9 Boundary conditions of the bottom-stiffened panel used in the present study

Location	Constraints		Edge conditions
	Translational	Rotational	
A-A'	$T [0, 1, 0]$	$R [0, 1, 1]$	Simply supported
B-B'	$T [0, 1, 0]$	$R [1, 0, 1]$	Symmetric condition
C-C'	$T [1, 0, 0]$	$R [0, 1, 1]$	Symmetric condition

Note: $T [x, y, z]$ indicates the translational constraints, and $R [x, y, z]$ the rotational constraints, along the x -, y - and z -coordinates; “1” indicates a constraint, while “0” indicates no constraint.

The design landing force applied was 148.25 kN and the area of the landing force acting on the pancake was 90,000 mm². Six loading cases were considered to estimate the critical landing scenarios about the vertical direction of the aluminium pancake with regard to the landing force, as shown in Fig. 20.

3.3.3 Results of FE analysis

The structural safety of the developed aluminium pancake was analysed using the static analysis with regard to the landing force. Figs. 21 to 22 show the stress and displacement distribution of all cases. The safety check results based on FEA are summarised in Table 10. The allowable stress was calculated as allowable increase factor (1.33) × mesh size effect factor (1.4) × yield stress (260 MPa). As a result, the maximum safety ratio of the pancake was calculated to 0.32. Therefore, the developed aluminium pancake had a sufficient strength capacity to withstand the maximum landing force of 148.25 kN from a yield strength point of view. For a critical landing point of view, it was necessary to verify the structural behaviour using nonlinear structural analysis. Fig. 23 shows the nonlinear FEA results for Case I and II. It is clear that, as expected, the first yield point and buckling point occurred at Y-shaped webs. When the landing points were located in the middle of the pancake (Case II), yield points were equally distributed along two Y-shaped webs in the pancake. Therefore, for the new pancake design, the plate thickness and cross

Table 10 Safety check results

Load Cases	von-Mises stress [MPa]		Lateral displacement [mm]		Location
	Max.	Allowable	Max.	Allowable	
Case I	186		4.62		at web of pancake
Case II	171		8.00		at web of pancake
Case III	191	484	6.97	20.00	at web of AL girder
Case IV	145		1.58		at web of AL girder
Case V	156		6.12		at web of pancake
Case VI	209		7.68		at web of pancake

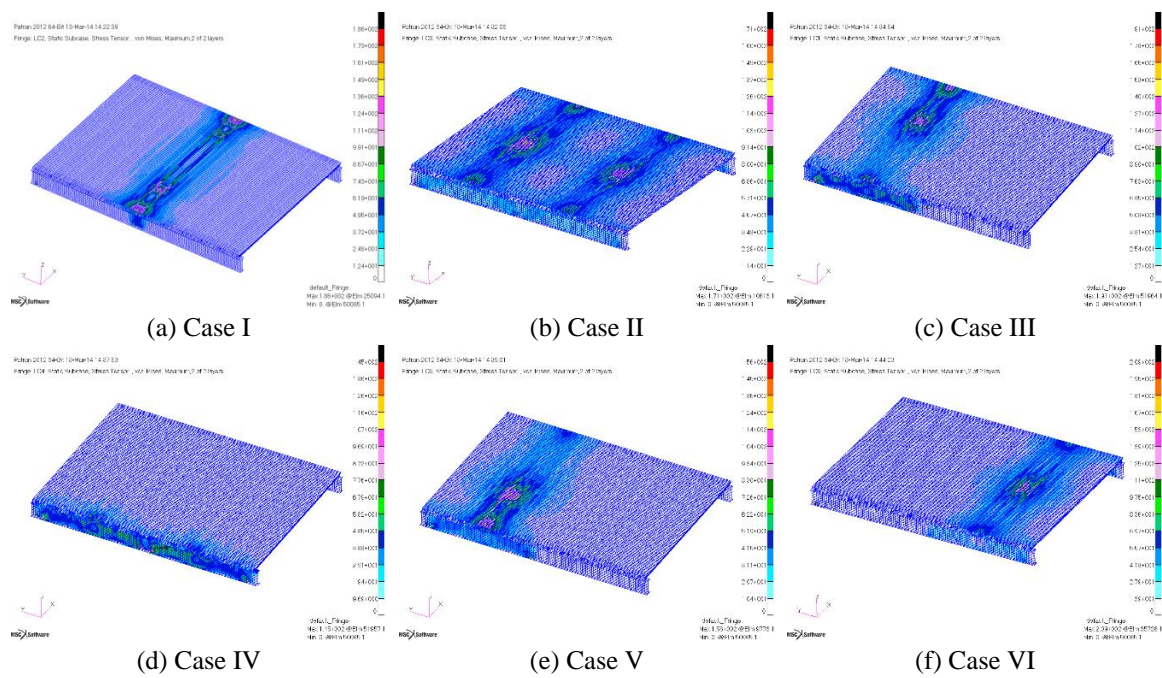


Fig. 21 Stress distribution of all load cases

section played a significant role when lateral compressive loads (landing load) were predominant. Also, it was observed that the yielding at the Y-shaped web occurred before the pancake buckling in both cases.

4. Effectiveness of the developed aluminium pancake

Three types of representative aluminium pancakes are widely used in offshore structures and vessels (Ha *et al.* 2015, Koo *et al.* 2014). In this study, the buckling strength of pancakes was compared using nonlinear static FE analysis. Fig. 24 shows the cross section and Table 14 shows the cross-section parameters of three existing pancakes. FEA models were analysed using nonlinear buckling analysis. The yielding of both of W-shaped and I-shaped pancakes occurred at

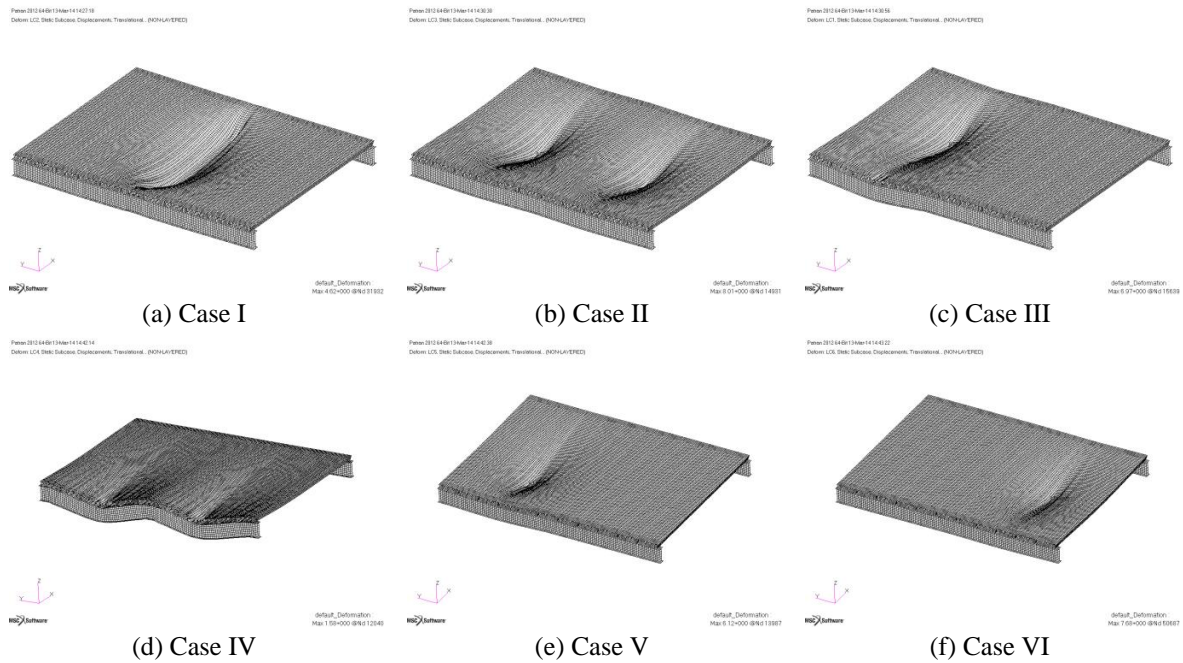


Fig. 22 Displacement distribution of all load cases

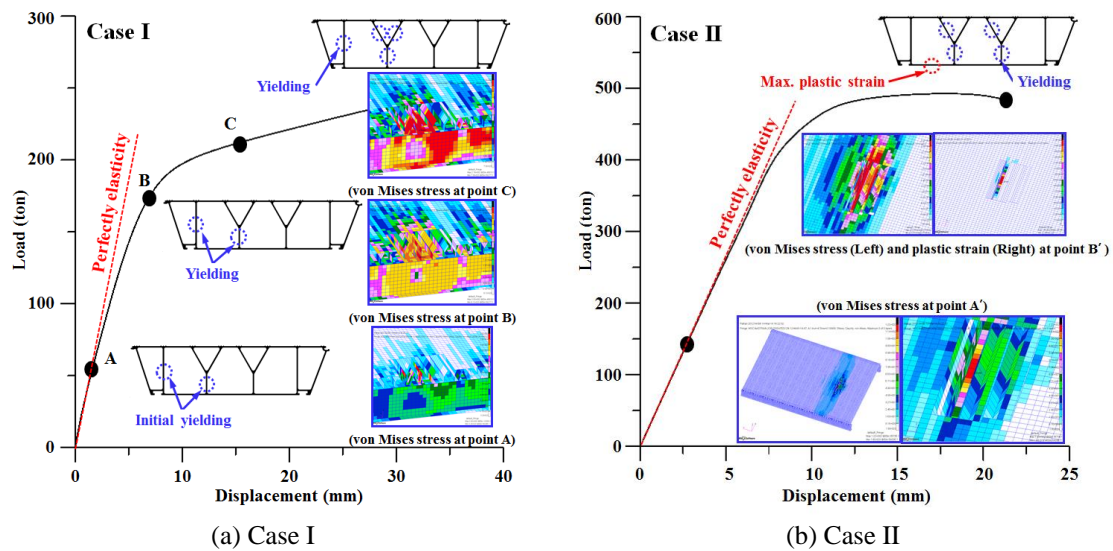


Fig. 23 Load vs. displacement curves and failure points of case I and II

the joint of the upper flange and the web before the flange buckling. In the case of the Y-shaped pancake, the yielding at the web of the pancake occurred before the flange buckling. These tendencies are different from the developed aluminium pancakes. A buckling capacity comparison between the existing and developed pancakes is shown in Fig. 25. The developed aluminium pancake shows the greatest buckling and ultimate strength capacity.

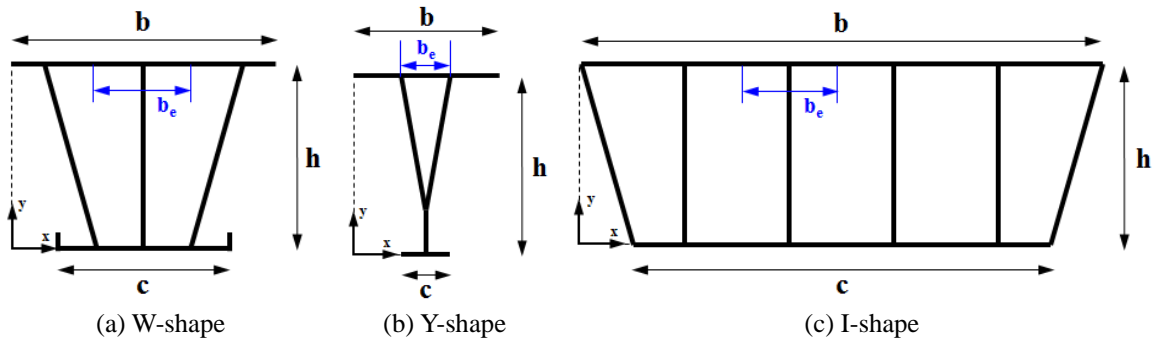


Fig. 24 Cross section of existing pancake

Table 14 Cross-section parameters of existing pancakes

Type	W-shape	Y-shape	I-shape
b (mm)	272.00	180.00	450.00
c (mm)	160.00	90.00	330.00
h (mm)	130.00	150.00	150.00
Area (mm ²)	3.83E+03	2.79E+03	6.13E+03
Slenderness (Flange/Web)	17.59/40.23	17.20/45.53	21.75/47.33
Moment of inertia about the x axis (I_{xx}) (mm ⁴)	1.00E+07	8.81E+06	2.25E+07
Moment of inertia about the y axis (I_{yy}) (mm ⁴)	1.61E+7	3.30E+6	1.03E+8
Centroid position along x axis (mm)	136.00	90.00	225.00
Centroid position along y axis (mm)	71.34	92.56	80.17

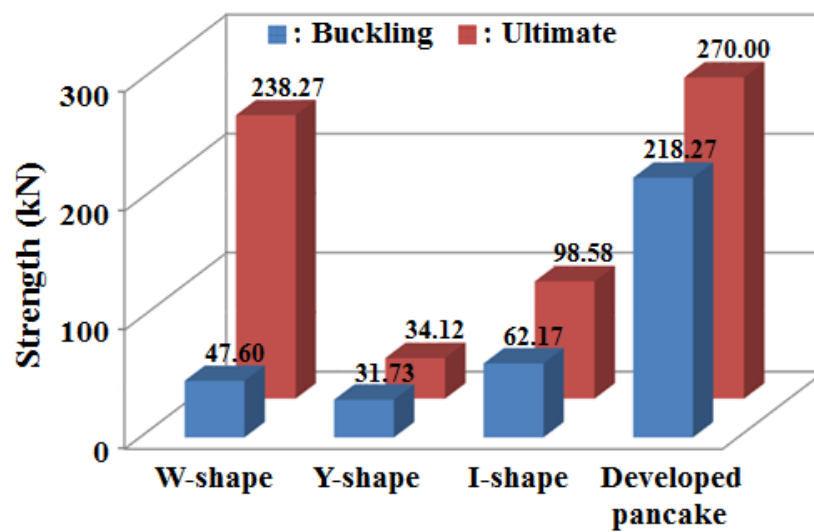


Fig. 25 Comparison of the buckling and ultimate strength

5. Conclusions

This study is the first to develop design procedures for Aluminium helideck pancake based on optimisation techniques using experimental studies, industrial regulations and nonlinear FEA. To validate and verify the procedure, a new aluminium pancake was developed and its buckling and ultimate capacity compared with those of existing pancakes.

The developed cross section of the aluminium pancake was 615 mm in breadth and 150 mm in height. In the initial stage of design, code check guidelines such as EN1999-1-1 were used, and then the structural safety of the initial design was verified by FEA considering the structural nonlinearities.

To validate the developed pancake, it was found that the developed aluminium pancake had sufficient strength of both yield and buckling strength. For verification with respect to evaluation by code, a series of FE analyses were performed. From the results, it was found that the buckling and ultimate strength of the developed aluminium pancake was 218.27 kN and 270.00 kN. Hence, the developed aluminium pancake had sufficient strength capacity to withstand the maximum landing force of 148.25 kN from in terms of buckling strength.

The buckling strength calculated from nonlinear static analyses for existing aluminium pancakes was compared with that of the developed aluminium pancake. Based on the comparison of the results, it was found that the pancake shape was the most important design parameter. The main reason being that it may be distributed the impact load, so that the new pancake design is stronger compared to existing pancakes.

The proposed design method could be helpful in the development of new aluminium helidecks based on optimisation techniques using experimental studies, industrial regulations and nonlinear FEA.

References

- Aalberg, A., Langseth, M. and Malo, K.A. (1998), "Ultimate strength of stiffened aluminium plates", Norwegian University of Science and Technology, Trondheim, Norway.
- American Petroleum Institute (2008), *API-RP-2L: Recommended Practice for Planning, Designing and Constructing Heliports for Fixed Offshore Platforms*, Washington, D.C., USA.
- CAP (2005), CAP 437: Offshore Helideck Landing Areas - Guidance on Standards, Flight Operations Department, Safety Regulation Group, Civil Aviation Authority, West Sussex, UK.
- Clarke, J.D. (1987), "Buckling of aluminium alloy stiffened plate ship structure", Ed. Narayanan, R., *Aluminium Structures-advances, Design and Construction*, Elsevier, Pennsylvania, USA.
- Čokorilo, O., Miroslavljević, P., Vasova, L. and Stojiljković, B. (2013), "Managing safety risks in helicopter maritime operations", *J. Risk Res.*, **16**(5), 613-624.
- DNV (2011), DNV-OS-C101: Design of Offshore Steel Structures, General (LRFD Method), Det Norske Veritas, Oslo, Norway.
- Elsayed, T., El-Shaib, M. and Gbr, K. (2016), "Reliability of fixed offshore jacket platform against earthquake collapse", *Ships Offshore Struct.*, **11**(2), 167-181.
- EN (2007), EN1999-1-1, Eurocode 9: Design of Aluminium Structures - Part 1-1: general structural rules, European Committee for Standardization, Brussels.
- Ha, Y., Park, J., Koo, J., Suh, Y., Seo, J., Shin, W. and Seo, Y. (2015), "Development of large-scaled SAFE helideck structure", *Proc. of 25th Inter. Conf. ISOPE*, Hawaii, USA, June.
- Hirdaris, S.E., Bai, W., Dessi, D., Ergin, A., Gue, X., Hermundstad, O.A., Huijsmans, R., Iijima, K., Nielsen, U.D., Parunov, J., Fonseca, N., Papanikolaou, A., Argyriadis, K. and Incecik, A. (2015), "Loads

- for use in the design of ships and offshore structures”, *Ocean Eng.*, **78**, 131-174.
- HSE (2012), *Offshore Helideck Design Guidelines*, Health and safety Executive, Aberdeen, UK.
- ICAO (2013), *Annex 14 Volume II Heliports and Heliports manual*, International Civil Aviation Organisation.
- ISO (2014), *ISO 19901-3: Petroleum and natural gas industries-Specific requirement for offshore structures-Part 3: topsides structure*, International Organization for Standardization, Geneva, Switzerland
- Koo, J., Park, J., Ha, Y., Jang, K., Suh, Y. (2014), “Nonlinear structural response analysis for aluminium helideck”, *Proc. of 24th Inter. Conf. ISOPE*, Busan, Korea, June.
- Kristensen, Q.H.H. and Moan, T. (1999), “Ultimate strength of aluminium plates under biaxial loading”, *Proc. of Fifth Inter. Conf. on Fast Sea Transportation*, New York, USA.
- Mascia, D. (2010), “Structural behaviour of landing deck marine vessel under dynamic actions of aircraft landing”, *Ships Offshore Struct.*, **5**(3), 267-282.
- Mentzoni, F. and Ertesvåg, I.S. (2015) “On turbulence criteria and model requirements for numerical simulation of turbulent flows above offshore helidecks”, *J. Wind Eng. Indus. Aerodyn.*, **142**, 164-172.
- NX Nastran (2012), *Manual of NX Nastran*, Siemens PLM Software, California, USA.
- Paik, J.K. and Duran, A. (2004), “Ultimate strength of aluminium plates and stiffened panels for marine structures”, *Marine Tech.*, **41**(3), 108-121.
- Park, D., Choi, S., Kim, J. and Lee, J. (2015) “Cryogenic mechanical behavior of 5000- and 6000-series aluminum alloys: Issues on application to offshore plants”, *Cryogen.*, **68**, 44-58.
- Raheem, S.E.A. (2016) “Nonlinear behaviour of steel fixed offshore platform under environmental loads”, *Ships Offshore Struct.*, **11**(1), 1-15.
- Shukla, A. and Misra, A. (2013), “Review of optimality criterion approach scope, limitation and development in topology optimization”, *Int. J. Adv. Eng. Tech.*, **6**(4), 1886-1889.
- TOSCA (2012), *TOSCA Structures 8.0. Manual of structural optimization*, Dassault systems, Courbevoie, France.
- UK CAA (2012), *CAP437: Standards for Offshore Helicopter Landing Areas, Guidance on Standards*, Seventh Edition, UK Civil Aviation Authority, West Sussex, UK.
- Wikipedia (2016), http://en.wikipedia.org/wiki/Airbus_Helicopters.
- Zha, Y., Moan, T. and Hanken, E. (2000), “Experimental and numerical study of torsional buckling of stiffeners in aluminium panels”, *Proc. of 5th Inter. Conf. ISOPE*, Seattle, USA, May.
- Zha, Y., Moan, T. and Hanken, E. (2001), “Ultimate strength of stiffened aluminium panels with predominantly torsional failure modes”, *Thin Wall. Struct.*, **39**, 631-648.